Lecture Notes in Electrical Engineering 1018

Chengbin Ma · Yiming Zhang ·
Siqi Li · Lei Zhao · Ming Liu ·
Pengcheng Zhang *Editors*

The Proceedings of 2022 International Conference on Wireless Power Transfer (ICWPT2022)

Springer

Lecture Notes in Electrical Engineering 1018

The book series *Lecture Notes in Electrical Engineering* (LNEE) publishes the latest developments in Electrical Engineering—quickly, informally and in high quality. While original research reported in proceedings and monographs has traditionally formed the core of LNEE, we also encourage authors to submit books devoted to supporting student education and professional training in the various fields and applications areas of electrical engineering. The series cover classical and emerging topics concerning:

- Communication Engineering, Information Theory and Networks
- Electronics Engineering and Microelectronics
- Signal, Image and Speech Processing
- Wireless and Mobile Communication
- Circuits and Systems
- Energy Systems, Power Electronics and Electrical Machines
- Electro-optical Engineering
- Instrumentation Engineering
- Avionics Engineering
- Control Systems
- Internet-of-Things and Cybersecurity
- Biomedical Devices, MEMS and NEMS

For general information about this book series, comments or suggestions, please contact leontina.dicecco@springer.com.

To submit a proposal or request further information, please contact the Publishing Editor in your country:

China

Jasmine Dou, Editor (jasmine.dou@springer.com)

India, Japan, Rest of Asia

Swati Meherishi, Editorial Director (Swati.Meherishi@springer.com)

Southeast Asia, Australia, New Zealand

Ramesh Nath Premnath, Editor (ramesh.premnath@springernature.com)

USA, Canada

Michael Luby, Senior Editor (michael.luby@springer.com)

All other Countries

Leontina Di Cecco, Senior Editor (leontina.dicecco@springer.com)

**** This series is indexed by EI Compendex and Scopus databases. ****

Chengbin Ma · Yiming Zhang · Siqi Li ·
Lei Zhao · Ming Liu · Pengcheng Zhang
Editors

The Proceedings of 2022 International Conference on Wireless Power Transfer (ICWPT2022)

Springer

Editors
Chengbin Ma
Shanghai Jiao Tong University
Shanghai, China

Siqi Li
Kunming University of Science
and Technology
Kunming, Yunnan, China

Ming Liu
Shanghai Jiao Tong University
Shanghai, China

Yiming Zhang
Fuzhou University
Fuzhou, Fujian, China

Lei Zhao
Chongqing University
Chongqing, China

Pengcheng Zhang
Tsinghua University
Beijing, China

ISSN 1876-1100 ISSN 1876-1119 (electronic)
Lecture Notes in Electrical Engineering
ISBN 978-981-99-0630-7 ISBN 978-981-99-0631-4 (eBook)
https://doi.org/10.1007/978-981-99-0631-4

This Springer imprint is published by the registered company Springer Nature Singapore Pte Ltd.
The registered company address is: 152 Beach Road, #21-01/04 Gateway East, Singapore 189721, Singapore

Contents

Quadrature Six-Coils Wireless Charging with High Misalignment Tolerance and Constant Voltage Output

Zhaowei Gong[1,2], Jingang Li[1,3](✉), Xiangqian Tong[1], and Ningchao Zhang[2]

[1] School of Electrical Engineering, Xi'an University of Technology, Xi'an 710054, China
gongzhaowei@xatu.edu.cn, {lijingang,xqtong}@xaut.edu.cn
[2] School of Electronic Information Engineering, Xi'an Technological University, Xi'an 710021, China
zhangningchao@xatu.edu.cn
[3] Huaibei Huaming Industrial Frequency Conversion Equipment Co., Ltd., Huaibei 235100, China

Abstract. Aiming at improving the operating range of the wireless charging system with misalignment tolerance, a design method based on parameter optimization of wireless charging with wide range misalignment and constant-voltage output was proposed. The mathematical model of the proposed six-coils hybrid compensation network were established, and the output characteristics between load and mutual inductances were analyzed. The DD2Q (Double-D Quadrature) pad was proposed, which is beneficial to eliminate cross coupling and realize independent output of each channel. The results show that the system output current deviation is less than 5% when the coupling pads vary from 20 mm to 140 mm, and the efficiency is up to 94%.

Keywords: Wireless charging · Misalignment tolerance · Constant voltage output

1 Introduction

Inductive Power Transfer (IPT) is a method of energy transmission through high-frequency alternating magnetic field coupling, which has the advantages of safety, reliability, environmental friendliness and convenient operation. At present, it has been successfully applied to electronic products, medical electronic equipment and electric vehicles. Coupling coil is an important element of wireless charging system. The misalignment between the coupling coil will decrease the output power and efficiency. Therefore, wide range anti-offset output capability has become an important indicator of wireless charging system [1–5].

Aiming at improving the anti-offset ability, the optimization design is mainly from closed-loop control, magnetic coupling structure and high-order compensation network [6, 7]. The anti-offset output system based on closed-loop control usually requires additional wireless communication devices, but the wireless communication delay will

C. Ma et al. (Eds.): ICWPT 2022, LNEE 1018, pp. 1–7, 2023.
https://doi.org/10.1007/978-981-99-0631-4_1

reduce the dynamic response of the system. DDQ coil structure, DD coil structure, I-type transmitting coil structure and 3D orthogonal coil structure were proposed in [8–11] to provide misalignment tolerance against coupling fluctuations. For example, a I-type transmitting coil is proposed in [9] to realize the fluctuation range of output voltage within 30% when the maximum offset in x direction is within 50%. A 3D orthogonal coil structure was presented in [11] to realize all-directional wireless charging, but the overall efficiency of the system is only 60%. Meanwhile, hybrid compensation network can also be used to provide better misalignment tolerance. A hybrid compensation network combining with LCC-LCC and S-S compensation network [12], could realize stable the power output when the system coupling coefficient varied from 0.2 to 0.3. However, this hybrid topology cannot operate without the secondary side. A series hybrid topology with the integrating compensating inductor into coupling coil was proposed in [13] to overcome the above mentioned issues. The operating principle of the hybrid compensation network was summarized in [14], and set up an experimental platform, which could limit the fluctuation range, when the coupling coefficient is 0.08–0.16. To sum up, the existing methods can achieve anti-offset wireless charging, but the range of coupling coefficient is relatively narrow. Considering different EVs, such as family cars, SUVs or trucks, the vertical height of the coupling coil is different, and the coupling coefficient varies widely, resulting in transmission power fluctuation and efficiency decline. Therefore, it is necessary to improve the operating range of vertical misalignment tolerance.

The six-coil hybrid topology is presented in this paper. Firstly, the output characteristics of the topological circuit are analyzed. Secondly, the magnetic coupling coil structure of DD2Q is proposed to realize the mutual inductance decoupling between the same side coils. Finally, the experimental results show that the six-coil hybrid topology can achieve a wide range of anti-offset constant-current output, and the maximum efficiency of the system can reach 94%.

2 The Proposed Hybrid IPT System

Figure 1 illustrates the six-coil hybrid topology circuit. Aiming at minimizing the VA rating, all resonant components should be tuned to the same angle frequency ω, therefore, we can get

$$\begin{cases} \omega^2 L_0 C_0 = \omega^2 L_1 \frac{C_0 C_1}{C_0 + C_1} = 1,\ \omega^2 L_7 C_7 = \omega^2 L_4 \frac{C_4 C_7}{C_4 + C_7} = 1 \\ \omega^2 L_2 C_2 = \omega^2 L_3 C_3 = \omega^2 L_6 C_6 = 1,\ \omega^2 L_8 C_8 = \omega^2 L_5 \frac{C_5 C_8}{C_5 + C_8} = 1 \end{cases} \quad (1)$$

Then, the KVL equations can be obtained as

$$\begin{bmatrix} Z_{00} & Z_{01} & Z_{02} & 0 & Z_{04} & 0 & 0 \\ Z_{10} & Z_{11} & Z_{12} & 0 & Z_{14} & 0 & Z_{16} \\ Z_{20} & Z_{21} & Z_{22} & 0 & 0 & Z_{25} & Z_{26} \\ 0 & 0 & 0 & Z_{33} & 0 & Z_{35} & 0 \\ Z_{40} & Z_{41} & 0 & 0 & Z_{44} & 0 & Z_{46} \\ 0 & 0 & Z_{52} & Z_{53} & 0 & Z_{55} & Z_{56} \\ 0 & Z_{61} & Z_{62} & 0 & Z_{64} & Z_{65} & Z_{66} \\ 0 & 0 & Z_{72} & 0 & 0 & 0 & Z_{75} \end{bmatrix} \begin{bmatrix} \dot{I}_0 \\ \dot{I}_1 \\ \dot{I}_2 \\ \dot{I}_3 \\ \dot{I}_4 \\ \dot{I}_5 \\ \dot{I}_7 \end{bmatrix} = \begin{bmatrix} \dot{U}_{\text{out}} \\ 0 \\ 0 \\ \dot{U}_{\text{out}} \\ 0 \\ 0 \\ 0 \\ \dot{U}_{\text{AC}} \end{bmatrix} \quad (2)$$

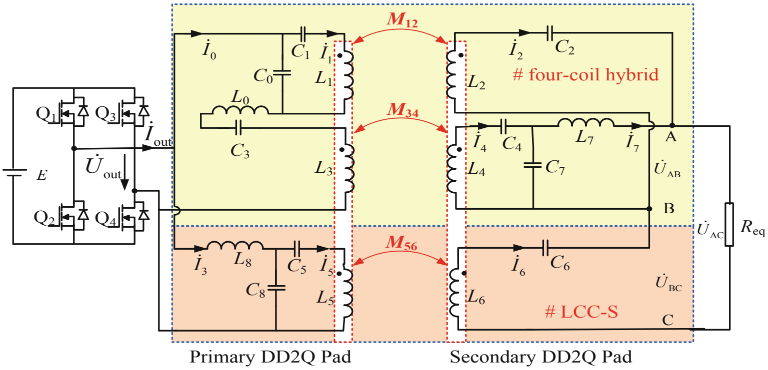

Fig. 1. Proposed six-coil hybrid IPT system.

where $Z_{00} = j\omega L_0 + (j\omega C_0)^{-1} + j\omega L_3 + (j\omega C_3)^{-1}$, $Z_{01} = Z_{10} = -(j\omega C_0)^{-1}$,
$Z_{02} = Z_{20} = -j\omega M_{23}$, $Z_{04} = Z_{40} = -j\omega M_{34}$, $Z_{11} = j\omega L_1 + (j\omega C_0)^{-1} + (j\omega C_1)^{-1}$,
$Z_{12} = Z_{21} = -j\omega M_{12} - j\omega M_{16}$, $Z_{14} = Z_{41} = -j\omega M_{14}$, $Z_{16} = Z_{61} = -j\omega M_{16}$,
$Z_{22} = j\omega L_2 + (j\omega C_2)^{-1} + R_{AC} + j\omega L_6 + (j\omega C_6)^{-1}$,$Z_{25} = Z_{52} = -j\omega M_{25} - j\omega M_{56}$,
$Z_{26} = Z_{62} = R_{AC} + j\omega L_6 + (j\omega C_6)^{-1}$, $Z_{33} = j\omega L_8 + (j\omega C_8)^{-1}$, $Z_{35} = Z_{53} = -(j\omega C_8)^{-1}$,
$Z_{44} = j\omega L_4 + (j\omega C_4)^{-1} + (j\omega C_7)^{-1}$, $Z_{46} = Z_{64} = -(j\omega C_7)^{-1}$,
$Z_{55} = j\omega L_5 + (j\omega C_5)^{-1} + (j\omega C_8)^{-1}$, $Z_{56} = Z_{65} = -j\omega M_{56}$,
$Z_{66} = j\omega L_7 + (j\omega C_7)^{-1} + R_{AC} + j\omega L_6 + (j\omega C_6)^{-1}$,$Z_{72} = Z_{76} = R_{AC}$.

In this paper, only the main mutual inductance is considered and the cross mutual inductance is ignored. Thus, we can get,

$$\dot{U}_{AC} = \frac{L_7 M_{12} \dot{U}_{out}}{L_0 L_7 + M_{12} M_{34}} + \frac{M_{56} \dot{U}_{out}}{L_8} \tag{3}$$

From (3), the output voltage of the load is related with resonant inductor L_0, L_7, L_8. If these parameters are well designed, the proposed IPT system can maintain stable voltage output.

3 Magnetic Coupler

Figure 2 shows the DD2Q pad in this paper, and the Magnetic inductance distribution is shown in Fig. 3. It is clear that the cross coupling occurs when the lateral misalignment happens, while there is only main coupling when the vertical misalignment happens. Therefore, the proposed DD2Q can be used in these applications, such as medical implant and AGVs, which may has wide vertical misalignment.

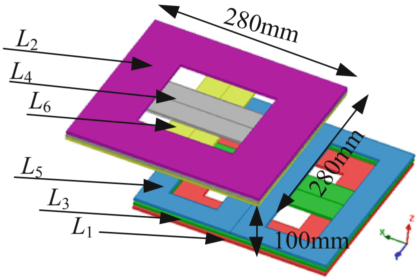

Fig. 2. DD2Q magnetic coupler

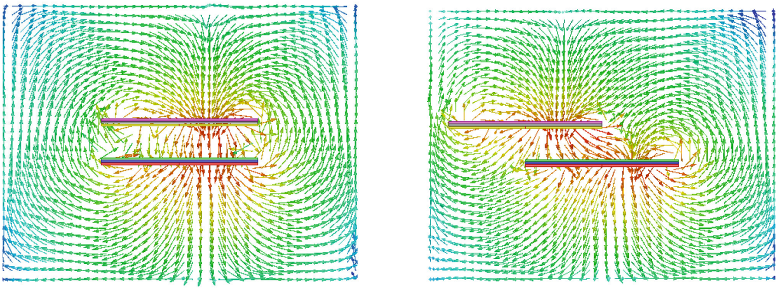

(a) at centrosymmetric position (b) at lateral offset position

Fig. 3. Magnetic inductance distribution of the DD2Q coil structure

4 Experimental Verification

Figure 4 shows the wireless charging experiment platform, where the electronic load is used to simulate the changes in battery charging process. And Table 1 is the specific experimental parameters are shown in Table 1.

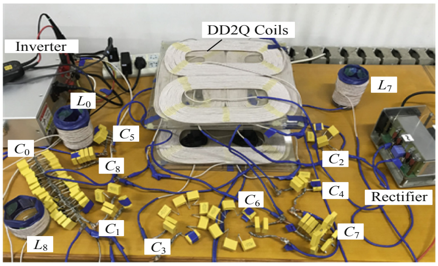

Fig. 4. Experiment platform

Figure 5(a) shows the output voltage curves with 80 Ω and 160 Ω load when vertical misalignment changes from 20 mm to 140 mm. It is obvious that the output voltage can remain relatively constant, The maximum output voltage is 104.5 V when the vertical

Table 1. The parameters

Parameter	Value	Parameter	Value
f	85 kHz	C_1	24.9 nF
L_1	150.1 μH	C_2	24.1 nF
L_2	149.8 μH	C_3	22.0 nF
L_3	160.1 μH	C_4	35.9 nF
L_4	160.2 μH	C_5	41.0 nF
L_5	160.1 μH	C_6	22.0 nF
L_6	160.1 μH	C_7	58.6 nF
L_7	60.2 μH	C_8	51.8 nF
L_8	70.2 μH	Air gap	20 mm–140 mm
C_0	388.4 nF	E	55 V

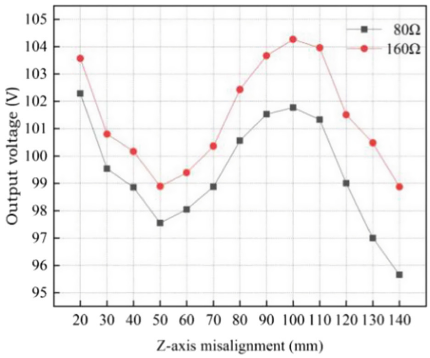

(a) output voltage

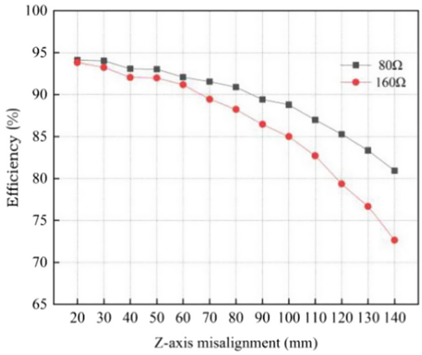

(b) efficiency

Fig. 5. Output voltage and efficiency curves at z-axis misalignment

misalignment reaches 100 mm, and the minimum output voltage is 95.66 V when the vertical misalignment reaches 140 mm. Figure 5(b) shows the system efficiency decreases when the vertical misalignment increases.

Figure 6 shows the experimental waveforms of different z-axis misalignment when the load resistance is 80 Ω. It can be obviously found that the variation of the output voltage is within 5%.

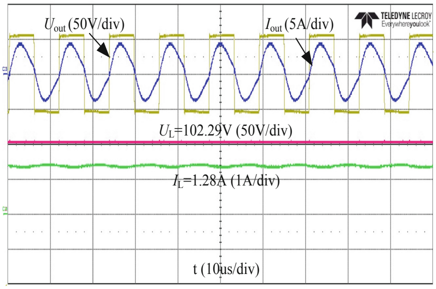

(a) at 20 mm Z-axis misalignment

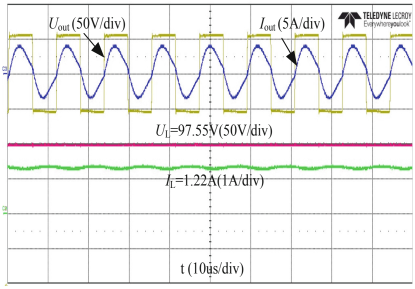

(b) at 50 mm Z-axis misalignment

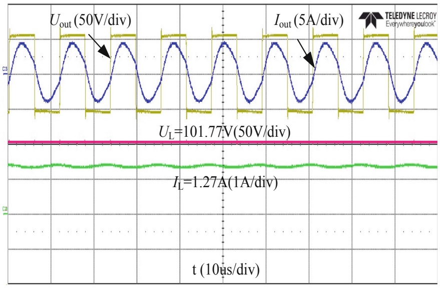

(c) at 100 mm Z-axis misalignment

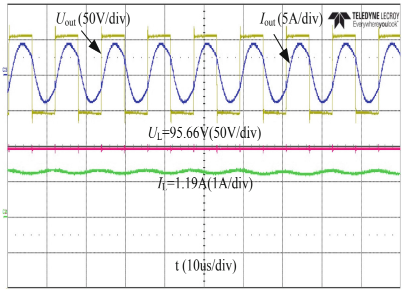

(d) at 140 mm Z-axis misalignment

Fig. 6. Experimental waveforms at $R_L = 80\ \Omega$

5 Conclusion

This paper presents a six-coil hybrid IPT topology. Firstly, the working characteristics of the system circuit are analyzed, and the variation rule of the output current is summarized. Secondly, DD2Q coupling coil structure is proposed to eliminate cross-coupling mutual inductance. Finally, the experimental results are consistent with the theoretical analysis.

Acknowledgements. This work was supported by the Key Research Project of Shaanxi Province of China under Grant 2022GY-310, and the Natural Science Foundation of Shaanxi Provincial Department of Education of China under Grant 20JK0688.

References

1. Mai, J., Wang, Y., Yao, Y., et al.: High-misalignment-tolerant IPT systems with solenoid and double D pads. IEEE Trans. Ind. Electron. **69**(4), 3527–3536 (2022)
2. Lee, Y., Han, S.: 2-D thin coil designs of IPT for wireless charging of automated guided vehicles. IEEE J. Emerg. Sel. Top. Power Electron. **10**(2), 2629–2644 (2022)
3. Li, Y., Du, H., He, Z., et al.: Robust control for the IPT system with parametric uncertainty using LMI pole constraints. IEEE Trans. Power Electron. **35**(1), 1022–1035 (2020)
4. Mai, J., Zeng, X., Yao, Y., et al.: Impedance analysis and design of IPT system to improve system efficiency and reduce output voltage or current fluctuations. IEEE Trans. Power Electron. **36**(12), 14029–14038 (2021)

5. Feng, H., Lukic, S.M.: Reduced-order modeling and design of single-stage LCL compensated IPT System for low voltage vehicle charging applications. IEEE Trans. Veh. Technol. **69**(4), 3728–3739 (2020)
6. Dai, X., Li, X., Li, Y., et al.: Maximum efficiency tracking for wireless power transfer systems with dynamic coupling coefficient estimation. IEEE Trans. Power Electron. **33**(6), 5005–5015 (2018)
7. Feng, H., Cai, T., Duan, S., et al.: An LCC-compensated resonant converter optimized for robust reaction to large coupling variation in dynamic wireless power transfer. IEEE Trans. Ind. Electron. **63**(10), 6591–6601 (2016)
8. Budhia, M., Boys, J.T., Covic, G.A., et al.: Development of a single-sided flux magnetic coupler for electric vehicle IPT charging systems. IEEE Trans. Ind. Electron. **60**(1), 318–328 (2013)
9. Park, C., Lee, S., Jeong, S.Y., et al.: Uniform power I-type inductive power transfer system with DQ-power supply rails for on-line electric vehicles. IEEE Trans. Power Electron. **30**(11), 6446–6455 (2015)
10. Yao, Y., Wang, Y., Liu, X., et al.: A novel unsymmetrical coupling structure based on concentrated magnetic flux for high-misalignment IPT applications. IEEE Trans. Power Electron. **34**(4), 3110–3123 (2019)
11. Zhang, Z., Zhang, B.: Angular-misalignment insensitive omnidirectional wireless power transfer. IEEE Trans. Ind. Electron. **67**(4), 2755–2764 (2020)
12. Zhao, L., Thrimawithana, D.J., Madawala, U.K.: Hybrid bidirectional wireless EV charging system tolerant to pad misalignment. IEEE Trans. Ind. Electron. **64**(9), 7079–7086 (2017)
13. Zhao, W., Qu, X., Lian, J., et al.: A family of hybrid IPT couplers with high tolerance to pad misalignment. IEEE Trans. Power Electron. **37**(3), 3617–3623 (2022)
14. Li, G., Ma, H.: A hybrid IPT system with high-misalignment tolerance and inherent CC–CV output characteristics for EVs charging applications. IEEE Trans. Power Electron. **10**(3), 3152–3161 (2022)

Inductively Coupled Power Transfer System Based Constant Voltage and Constant Current Charging for Rail Transit System

Jixin Yang[1,2](✉), Liming Shi[1], Zhenggang Yin[1], and Wenjing Tang[1,2]

[1] Key Laboratory of Power Electronics and Electric Drive, Institute of Electrical Engineering, Chinese Academy of Sciences, Beijing 100190, China
{jixiny,limings,yzhg,twj}@mail.iee.ac.cn
[2] University of Chinese Academy of Sciences, Beijing 100049, China

Abstract. This paper focus on the constant voltage (CV) and constant current (CC) charging mode for rail transit energy storage by inductively coupled power transfer (ICPT) system. Firstly, the mathematical model of ICPT system based on LCC-S compensation network is established and analyzed, then a method of switching the parallel compensation capacitor of primary side to realize the switching of CV and CC charging mode is proposed in this paper, the zero voltage switching (ZVS) of MOSFETs can be realized in either CV or CC charging mode, and the method has the advantages of simple operation and high reliability. Finally, the simulation results are presented to verify the feasibility of the proposed method.

Keywords: Constant voltage · Constant current · Rail transit system · Inductively coupled power transfer system · Zero voltage switching

1 Introduction

At present, the third rail or overhead line and pantograph are the main power supply methods for rail transit system. However, these power supply methods have problems such as friction, electric sparks, electric shock risks and higher maintenance costs [1]. Therefore, the ICPT system has become an alternative to rail transit system power system power supply.

The LCC-S compensation network has better advantages for ICPT charging system, such as constant transmitting coil current, high efficiency and low losses [2]. Another advantage for its application in rail transit system is the reduction of the total weight of the vehicle, because only one compensation capacitor is needed.

The battery is the most commonly load as the energy storage in the rail transit system [3]. The battery charging process is mainly divided into two modes: CC charging mode and CV charging mode as shown in Fig. 1. First, the CC charging mode is used. When the battery voltage reaches the setting value, then the CV charging mode needs to be used. When the charging current is reduced to the charging cut-off current, the battery charging ends. The alternative CC and CV charging mode will prolong the

C. Ma et al. (Eds.): ICWPT 2022, LNEE 1018, pp. 8–17, 2023.
https://doi.org/10.1007/978-981-99-0631-4_2

service life of the battery, and it is also important to the safety of the ICPT system. Therefore, it is necessary to switch between the CC charging mode and CV charging mode corresponding to the ICPT system used in the rail transit system.

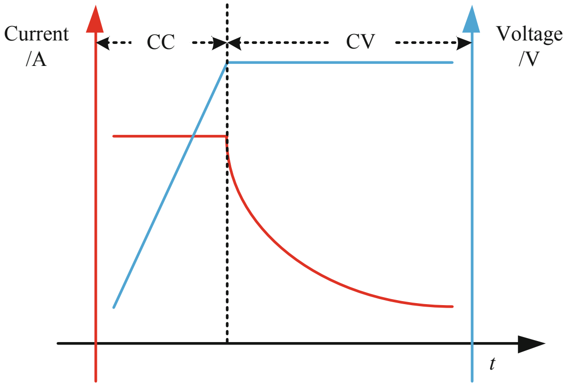

Fig. 1. Battery charging process.

In order to realize the switching of CV and CC charging mode of the ICPT system, a method of switching working frequency of the inverter is proposed in [4, 5]. This method doesn't require wireless communication, but this method is easy to cause the instability of the ICPT system with frequency bifurcation. In [6, 7], the closed-loop control method is adopted to realize the CV or CC charging mode of ICPT system, but closed-loop control method needs to transmit the voltage or current signal to the primary side, the data signal may be interfered by the energy signal, which will affect control accuracy. Meanwhile, the stability of the system using the closed-loop control also needs further research. In [8–10], a method of changing primary side or secondary side compensation structure is adopted, but more switching devices and compensation devices are used in this method, and the switching process between CV and CC charging mode is more complex.

In this paper, the ICPT system based on LCC-S compensation network is researched. First, the mathematical model of the system is established, and the conditions for the system to realize the CV and CC mode are obtained through analysis. Then, the method of switching parallel compensation capacitor on the primary side is proposed, the ZVS of the MOSFETs can be realized. Finally, the feasibility of the proposed method is verified through simulation results.

2 Topology of ICPT System

The topology of ICPT system is shown in Fig. 2. V_{dc} is the input dc voltage, V_{ab} and V_{cd} are the input and output voltages of the compensation network, respectively, V_o is the output dc voltage, I_1 is the input current of the compensation network, I_p and I_s are the current of the transmitting coil and receiving coil, respectively. L, C, C_1, C_p and L_p are formed primary side of compensation network while L_s and C_s are formed secondary side of the compensation network. r_p and r_s are the inner resistance, M is the mutual inductance, C_o is the output capacitor, R is the load, S_1 ~ S_4 are the MOSFETs of the inverter, D_1 ~ D_4 are the diodes of the rectifier.

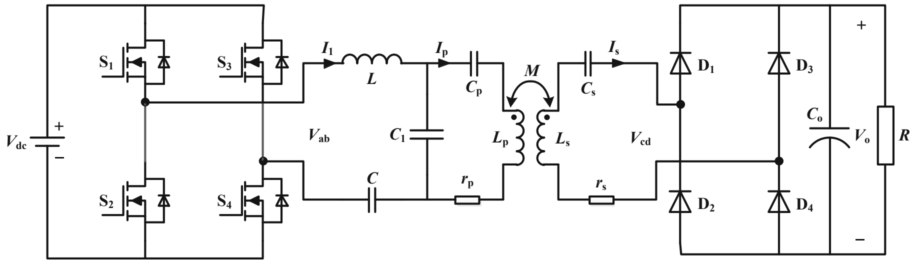

Fig. 2. Topology of ICPT system.

If r_p and r_s are ignored, the equivalent circuit of the ICPT system is shown in Fig. 3. Each parameter in Fig. 3 is expressed as (1).

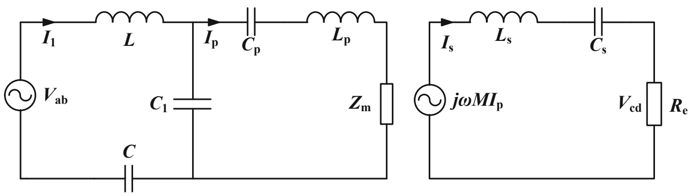

Fig. 3. Equivalent circuit of the ICPT system.

$$\begin{cases} V_{ab} = 2\sqrt{2}V_{dc}/\pi \\ Z_m = (\omega M)^2/(R_e + j\omega L_s + 1/j\omega C_s) \\ R_e = 8R/\pi^2 \\ V_{cd} = 2\sqrt{2}V_o/\pi \end{cases} \tag{1}$$

where ω is the resonant angular frequency of the system, Z_m is the reflection impedance, R_e is the ac equivalent resistance.

Let $Z_{eq} = j\omega L + 1/j\omega C$, $Z_C = 1/j\omega C_1$, $Z_p = j\omega L_p + 1/j\omega C_p$ and $Z_s = j\omega L_s + 1/j\omega C_s$, so the impedance of the primary side can be expressed as follows:

$$Z_{in} = Z_{eq} + Z_C/(Z_p + Z_m) = \frac{Z_{eq}(Z_C + Z_p + Z_m) + Z_C(Z_p + Z_m)}{Z_C + Z_p + Z_m} \tag{2}$$

So, I_1, I_p, I_s and V_{cd} can be expressed as follows,

$$I_1 = \frac{V_{ab}}{Z_{in}} = \frac{Z_C + Z_p + Z_m}{Z_{eq}(Z_C + Z_p + Z_m) + Z_C(Z_p + Z_m)} V_{ab} \tag{3}$$

$$I_{\mathrm{p}} = \frac{Z_{\mathrm{C}}}{Z_{\mathrm{C}} + Z_{\mathrm{p}} + Z_{\mathrm{m}}} I_1 = \frac{Z_{\mathrm{C}}}{Z_{\mathrm{eq}}(Z_{\mathrm{C}} + Z_{\mathrm{p}} + Z_{\mathrm{m}}) + Z_{\mathrm{C}}(Z_{\mathrm{p}} + Z_{\mathrm{m}})} V_{\mathrm{ab}} \tag{4}$$

$$I_{\mathrm{s}} = \frac{j\omega M}{Z_{\mathrm{s}} + R_{\mathrm{e}}} I_{\mathrm{p}} = \frac{j\omega M Z_{\mathrm{C}}}{(Z_{\mathrm{s}} + R_{\mathrm{e}})Z_{\mathrm{eq}}(Z_{\mathrm{C}} + Z_{\mathrm{p}} + Z_{\mathrm{m}}) + (Z_{\mathrm{s}} + R_{\mathrm{e}})Z_{\mathrm{C}}(Z_{\mathrm{p}} + Z_{\mathrm{m}})} V_{\mathrm{ab}} \tag{5}$$

$$V_{\mathrm{cd}} = I_{\mathrm{s}} R_{\mathrm{e}} = \frac{j\omega M Z_{\mathrm{C}} R_{\mathrm{e}}}{(Z_{\mathrm{s}} + R_{\mathrm{e}})Z_{\mathrm{eq}}(Z_{\mathrm{C}} + Z_{\mathrm{p}} + Z_{\mathrm{m}}) + (Z_{\mathrm{s}} + R_{\mathrm{e}})Z_{\mathrm{C}}(Z_{\mathrm{p}} + Z_{\mathrm{m}})} V_{\mathrm{ab}} \tag{6}$$

3 Analysis of CV and CC Charging Mode

3.1 CV Charging Mode

When the conditions shown in (7) are satisfied by the ICPT system, the CV charging mode of the ICPT system can be realized.

$$\begin{cases} Z_{\mathrm{eq}} + Z_{\mathrm{C}} = 0 \\ Z_{\mathrm{p}} + Z_{\mathrm{C}} = 0 \\ Z_{\mathrm{s}} = 0 \end{cases} \tag{7}$$

So, the impedance of the system in CV charging mode can be expressed as:

$$Z_{\mathrm{in\_CV}} = \frac{Z_{\mathrm{C}} Z_{\mathrm{p}}}{Z_{\mathrm{m}}} = \frac{R_{\mathrm{e}}}{(\omega^2 M C)^2} \tag{8}$$

It can be seen from (8), the impedance $Z_{\mathrm{in\_CV}}$ is resistive. In order to realize ZVS of MOSFETs, the impedance of the system needs to be designed to be slightly inductive.

In CV charging mode, V_{cd} can be expressed as follows:

$$V_{\mathrm{cd}} = \frac{\omega M}{\omega L_{\mathrm{p}} - 1/\omega C_{\mathrm{p}}} V_{\mathrm{ab}} \tag{9}$$

The curves of V_{cd} with operation frequency f under different load are shown in Fig. 4, and the ICPT system parameters are shown in Table. 1. As can be seen from Fig. 4, when the working frequency is 30 kHz, the CV charging mode of the ICPT system can be realized.

3.2 CC Charging Mode

On the basis of (5), I_{s} can be further derived as follows:

$$I_{\mathrm{s}} = \frac{j\omega M Z_{\mathrm{C}}}{(Z_{\mathrm{s}} + R_{\mathrm{e}})[Z_{\mathrm{eq}}(Z_{\mathrm{C}} + Z_{\mathrm{p}}) + Z_{\mathrm{C}} Z_{\mathrm{p}}] + (\omega M)^2 Z_{\mathrm{eq}} + (\omega M)^2 Z_{\mathrm{C}}} V_{\mathrm{ab}} \tag{10}$$

When the condition shown in (11) is satisfied by the ICPT system, the CC charging mode of the ICPT system can be realized.

$$Z_{\mathrm{eq}}(Z_{\mathrm{C}} + Z_{\mathrm{p}}) + Z_{\mathrm{C}} Z_{\mathrm{p}} = 0 \tag{11}$$

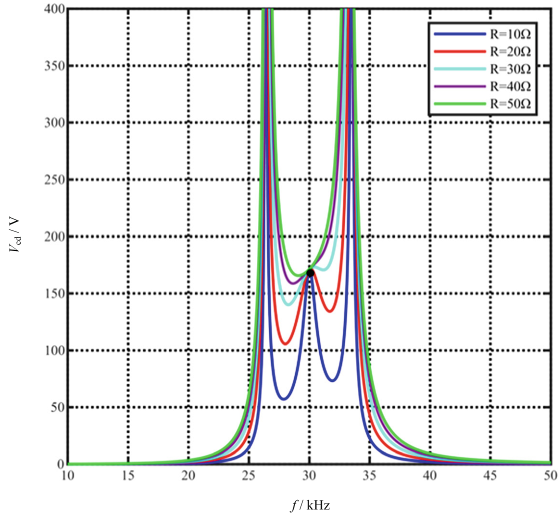

Fig. 4. Curves of V_{cd} with f under different load.

Table 1. Parameters of the ICPT system.

Symbol	Value	Symbol	Value
V_{dc}	100 V	L	62 μH
C	0.52 μF	C_1	3.57 μF
L_p	22.14 μH	C_p	1.97 μF
r_p	0.033 Ω	L_s	980 μH
C_s	28.71 nF	r_s	0.495 Ω
M	15 μH	C_o	2000 μF

To simplify the structure of the ICPT system, only one part of the system is modified in this paper, so there are three solutions are shown in (12), (13) and (14), respectively.

$$Z_C = -\frac{Z_{eq}Z_p}{Z_{eq} + Z_p} \tag{12}$$

$$Z_p = -\frac{Z_{eq}Z_C}{Z_{eq} + Z_C} \tag{13}$$

$$Z_{eq} = -\frac{Z_pZ_C}{Z_p + Z_C} \tag{14}$$

However, according to (7), in CV charging mode, $Z_{eq} + Z_C = 0$, $Z_p + Z_C = 0$, which will result in no solution to (13) and (14). Therefore, (12) is the only selection for the ICPT system to realize the CC charging mode in this paper.

So, on the basis of (7) and (12), in CC charging mode, the capacitance of the parallel compensation capacitor C_a can be derived as follows:

$$C_a = C_1 \tag{15}$$

So, the impedance of the system in CC charging mode can be expressed as:

$$Z_{in\_CC} = \frac{-Z_C Z_m}{2Z_m - Z_C} = \frac{(\omega M)^2 R_e + j2\omega C_1 (\omega M)^4}{4(\omega C_1)^2 (\omega M)^4 + R_e^2} \tag{16}$$

It can be seen from (16), the impedance Z_{in_CC} is inductive, so ZVS of MOSFETs can be realized.

In CC charging mode, I_s can be expressed as:

$$I_s = -j\frac{V_{ab}}{\omega M} \tag{17}$$

The curves of I_s with operation frequency f under different load are shown in Fig. 5. As can be seen from Fig. 5, when parallel compensation capacitor C_a is added, when the working frequency is 30 kHz, the CC charging mode of the ICPT system can be realized.

Therefore, the topology of ICPT system that can switch between CV and CC charging mode is shown in Fig. 6. When switch S_a is turned off, the CV charging mode can be realized, when S_a is turned on, the CC charging mode can be realized.

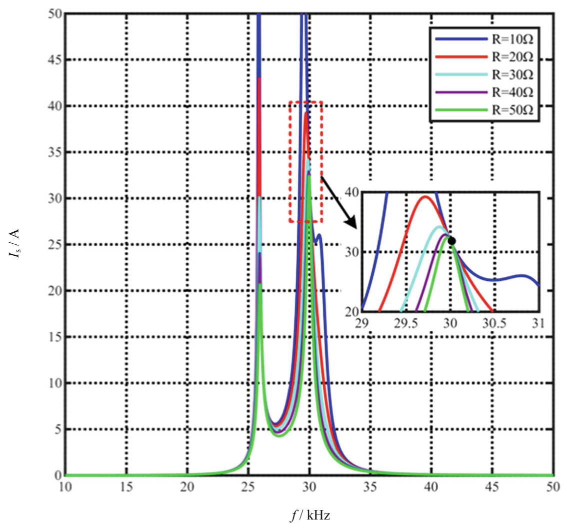

Fig. 5. Curves of I_s with f under different load.